engineering proceedings

MDPI

Proceeding Paper

Integrating Additive Manufacturing Constraints into the Conceptual Design of a Modular UAV †

Eleftherios Karatzas [1], Emmanouil Georgantakis [1] and Dimitrios Stamatelos [2,*]

[1] Department of Mechanical Engineering & Aeronautics, University of Patras, University Campus, 26504 Rion-Patras, Greece
[2] Laboratory of Strength of Materials, Division of Aeronautics, Applied Mechanics and Infrastructure, Hellenic Air Force Academy, Dekeleia Air Base-Attiki, 13671 Athens, Greece
* Correspondence: dimitrios.stamatelos@hafa.haf.gr
† Presented at The 1st International Online Conference on Aerospace (IOCAE 2026), 16–17 April 2026; Available online: https://sciforum.net/event/IOCAE2026.

Abstract

Conceptual design of small UAVs for tactical ISR missions is often complicated by the disconnect between early-stage aerodynamic sizing and the manufacturing and deployment constraints that emerge later in the design process. This work presents an iterative conceptual design framework in which additive manufacturing, modular assembly, and field-deployment constraints are introduced directly into the preliminary sizing loop. Mission requirements are first translated into aerodynamic sizing parameters using established conceptual design relations, leading to a representative feasible design point with a wing loading of approximately 20 kg/m^2 and an aspect ratio of approximately 9. These parameters are transferred to a parametric OpenVSP model, where the configuration is refined against manufacturing and integration constraints including printable component dimensions, wing segmentation, carbon-spar integration, subsystem packaging, and detachable interfaces. Structural feasibility is assessed through finite element analysis of the representative wing structure, incorporating printed PLA components and carbon-fiber reinforcement, and providing stiffness-based feedback during the conceptual iterations. The resulting workflow therefore links mission analysis, aerodynamic sizing, parametric geometry generation, manufacturing-driven configuration refinement, and structural assessment within a single conceptual design process. The representative UAV application demonstrates that manufacturing and deployment constraints influence the feasible geometry, modular arrangement, and internal structural configuration from the conceptual design stage, rather than being treated as downstream fabrication considerations.

Keywords: conceptual UAV design framework; additive manufacturing constraints; modular UAV; parametric design; structural feasibility assessment; field deployment

Check for updates

Academic Editors: Stephen Whitmore and Norman M. Wereley

Published: 19 November 2026

Copyright: © 2026 by the authors. Licensee MDPI, Basel, Switzerland. This article is an open access article distributed under the terms and conditions of the Creative Commons Attribution (CC BY) license.

1. Introduction

Unmanned Aerial Vehicles (UAVs) are increasingly employed in civilian and military Intelligence, Surveillance and Reconnaissance (ISR) missions, where low cost, rapid deployment, and operational flexibility are important design requirements. For small-scale tactical operations, Class I fixed-wing or rotary-wing UAVs are commonly used depending on mission duration, deployment requirements, and operational constraints [1]. In field-deployable applications, fixed-wing configurations remain particularly attractive due to their aerodynamic efficiency and extended endurance capabilities. However, such platforms must

also satisfy practical operational constraints, including hand-launch capability, compact transportation, rapid assembly, and operation with minimal external support equipment.

Conventional conceptual UAV design methodologies primarily focus on mission sizing, aerodynamic performance, and stability analysis [2–5]. In practice, however, fabrication and deployment constraints frequently emerge later in the design process, often requiring redesign iterations during prototyping and integration. This issue becomes more pronounced for small UAVs manufactured using additive manufacturing techniques and commercial off-the-shelf (COTS) subsystems, where limitations associated with printable geometries, modular assembly, internal packaging, and structural reinforcement directly influence the feasible configuration.

In small UAV platforms, the reduced internal volume and the integration of electrical propulsion systems, avionics, and payload components impose additional geometric and structural constraints during preliminary design. Furthermore, the use of 3D-printed polymer structures combined with carbon-fiber reinforcements introduces manufacturing-related limitations associated with printing orientation, structural stiffness, and detachable interfaces. If such constraints are not considered early, a significant redesign effort may be required during later development stages.

The present work proposes a conceptual UAV design framework in which manufacturing, modularity, and deployment constraints are integrated directly into the preliminary sizing process. Mission-driven sizing relations are coupled with parametric geometry generation and simplified structural assessment to evaluate candidate configurations under both aerodynamic and fabrication-related constraints. The methodology focuses on small modular UAVs, Figure 1, intended for tactical ISR missions and aims to support rapid prototyping and field deployment while reducing redesign iterations during development.

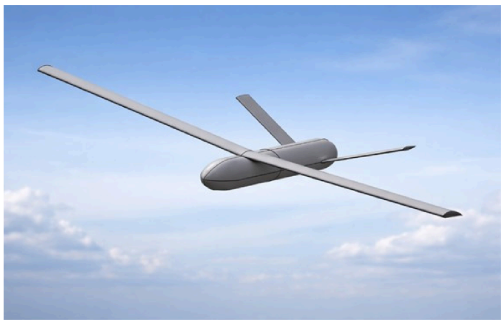


Figure 1. Concept design of the presented UAV.

2. Mission Definition and UAV Requirement Derivation

2.1. Mission Scenario and Operational Concept

The UAV is intended for tactical ISR missions, including target validation and battlefield observation. The platform is designed for rapid field deployment and operation by a single operator under limited logistical support.

Mission requirements impose several operational constraints on the configuration. The UAV must be compact enough for transportation in a military backpack, capable of hand launch, and able to operate without dedicated launch or recovery equipment. In addition, the platform should support modular payload integration to accommodate different sensor configurations based on mission requirements.

The representative UAV considered in this study serves as an application case for demonstrating the proposed conceptual design methodology under a realistic set of mission, manufacturing, and deployment requirements. It is therefore used to assess the applicability of the framework rather than as a baseline for comparative design optimization.

https://doi.org/10.3390/engproc2026142025

2.2. Mission Profile and UAV Requirements

Based on the operational scenario, the UAV mission profile is defined in terms of flight duration, velocity, range, and operating altitude. The resulting mission phases are summarized in Table 1.

Table 1. Mission profile of the UAV and subphase analysis.

Description	Time	Velocity	Range	Altitude (MSL)
Take-off	0.030 h	To be determined in a later stage	0 km (take off point)	0 m
Climb	0.046 h	Vertical: 6 m/s	0 km (over launch point)	1000 m
Cruise	0.091 h	Cruise: 110 km/h	10 km	1000 m
Loiter	0.500 h	To be determined in a later stage	0 km (over point of interest)	1000 m
Cruise	0.091 h	Cruise: 110 km/h	10 km	1000 m
Descent	0.046 h	Vertical: 6 m/s	0 km (over landing point)	1000 m
Land	0.050 h	To be determined in a later stage	0 km (landing point)	0 m
Total flight time	0.854 h		Total range	20 km

The corresponding preliminary UAV-level requirements are subsequently derived and used as inputs for the conceptual sizing process. These requirements include endurance, cruise velocity, payload capacity, climb performance, and operational altitude constraints, as summarized in Table 2.

Table 2. Initial requirements of the UAV.

Symbol	Description	Value
E	Endurance (hours) for loiter	0.500
$E_{runtime}$	Total flight time (hours)	0.854
R	Range (km)	20
W	Initial Target MTOM (kg)	2.8
W_{PL}	Desired payload mass of the UAV (kg)	0.3
V_{cr}	Desired cruise velocity (km/h)	95
V_{max}	Desired max velocity (km/h)	110
V_s	Desired stall speed (km/h)	60
V_{V_c}	Desired rate of climb velocity (m/s)	6
V_{V_d}	Desired rate of descent (m/s)	6
h_c	The required climb altitude (m)	1000
h_d	Required descent altitude (m)	0
FL_{LOWER}	Lower altitude of the mission (m)	0
FL_{HIGHER}	Higher altitude of the mission (m)	1000
$FL_{TAKEOFF}$	Take-off altitude (m)	0
$FL_{LANDING}$	Landing altitude (m)	0

2.3. Derived UAV-Level Requirements

2.3.1. Conceptual Design Phase

The preliminary sizing methodology follows conventional small-UAV conceptual sizing practice [2–6]. The calculations were implemented in an in-house spreadsheet-based sizing environment (Figure A1, Appendix A). Related applications of similar sizing methodologies to foldable UAV configurations are reported in [7–9].

Since the UAV is electrically powered, battery-based sizing relations were employed instead of the classical Breguet endurance formulation. Initial estimates of maximum take-

off mass were obtained iteratively using the Battery Mass Function (BMF) methodology [2] according to:

$$W_{calculated} = \frac{W_{payload}}{1 - BMF_{factor} - \frac{W_{empty}}{W_guess}}, \quad (1)$$

The resulting weight convergence obtained from the iterative sizing process is presented in Figure 2.

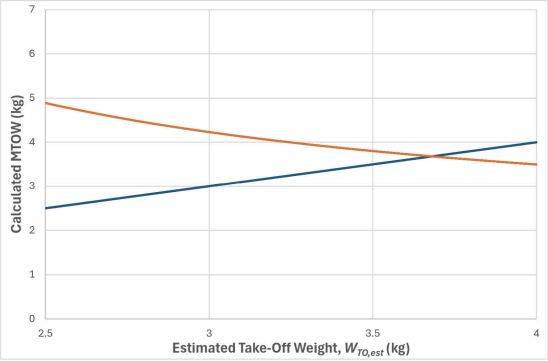


Figure 2. Weight convergence obtained from the spreadsheet-based sizing environment.

The iterative weight estimation converged at approximately 3.7–3.8 kg. This value represents the resulting estimated take-off mass obtained from the sizing procedure, whereas the 2.8 kg value reported in Table 2 was an initial target MTOM used at the beginning of the conceptual design process rather than a fixed constraint.

The feasible conceptual design region was subsequently identified through conventional wing-loading (W/S) and power-loading (W/P) design constraints derived from cruise, stall, climb, and maneuvering requirements (Figure 3). The selected design point corresponded approximately to $W/P = 4$ kg/kW and $W/S = 20$ kg/m^2.

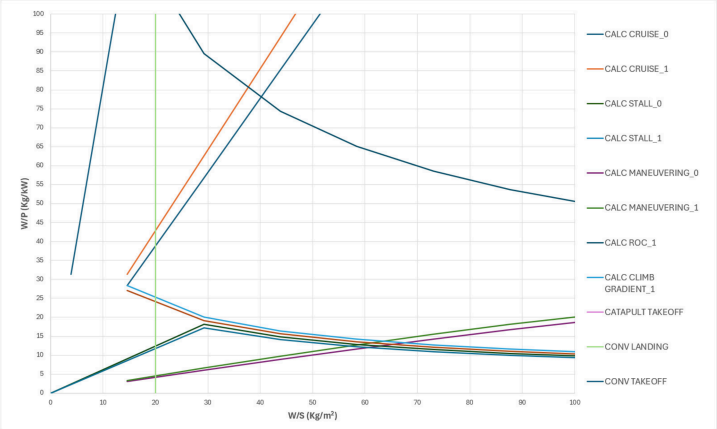


Figure 3. Wing-loading and power-loading constraint analysis obtained from the spreadsheet-based sizing environment.

A moderate aspect ratio of approximately 9 was selected as a compromise between aerodynamic efficiency, structural simplicity, transportability, and compatibility with segmented 3D-printed wing construction. The resulting sizing outputs were subsequently used as inputs for the preliminary geometric design phase.

These values define the baseline sizing outcome of the conceptual design stage and provide the aerodynamic and geometric starting point for the subsequent manufacturing-constrained configuration refinement.

2.3.2. Preliminary Design Phase

The preliminary geometric design focused on the wing and tail configuration, which directly influence the longitudinal and directional stability characteristics of the UAV. Stability requirements were evaluated using conventional aircraft design relations [2,4,5], while additive manufacturing and subsystem integration considerations simultaneously constrained the geometry. The resulting preliminary stability and configuration parameters are summarized in Table A1 (Appendix B).

In addition to aerodynamic performance, the wing and fuselage geometry had to satisfy practical fabrication constraints, including printable component dimensions, integration of carbon-fiber spars, and sufficient internal volume for avionics, servos, and electrical subsystems. A conventional tail configuration was initially sized and subsequently adapted to a vee-tail arrangement following the methodology presented in [10].

The resulting parametric geometry was generated in OpenVSP 3.40.0 Release [11,12] and used as the basis for the subsequent structural assessment phase. A representative preliminary configuration is presented in Figure 4.

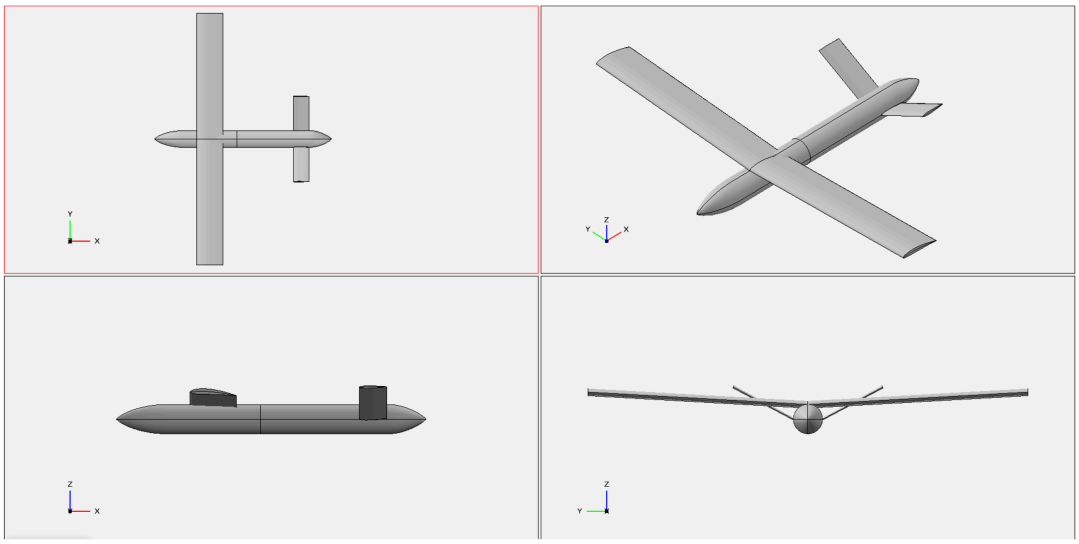


Figure 4. Preliminary UAV geometry generated through the parametric conceptual design framework.

Before proceeding to the structural assessment phase, the V–n diagram was evaluated to define the representative design load cases for the conceptual structural analysis.

3. Additive-First Conceptual Design Framework

3.1. Design Philosophy

Conventional UAV conceptual design workflows primarily focus on mission-driven sizing and aerodynamic performance, while manufacturing and deployment considerations are often introduced at later stages of the design process. In practice, this sequential approach may lead to redesign iterations during prototyping and subsystem integration, particularly for small UAV platforms manufactured using additive manufacturing techniques. Similar Design-for-Additive-Manufacturing (DfAM) methodologies emphasize the early integration of fabrication and assembly constraints during concept generation to reduce redesign iterations during downstream development stages [13–15].

The present work adopts an additive-first design philosophy in which manufacturing, modularity, and deployment constraints are introduced directly into the conceptual sizing stage before geometry finalization. As a result, candidate configurations are evaluated

not only with respect to aerodynamic and mission requirements, but also according to fabrication feasibility, subsystem integration, and field-deployment constraints.

The proposed framework combines preliminary sizing, parametric geometry generation, and simplified structural assessment within an iterative design process intended for rapid UAV prototyping and deployment.

3.2. Conceptual Design Workflow

The proposed framework integrates mission analysis, preliminary sizing, parametric geometry generation, manufacturing constraints, and simplified structural assessment within an iterative conceptual design loop, Figure 5.

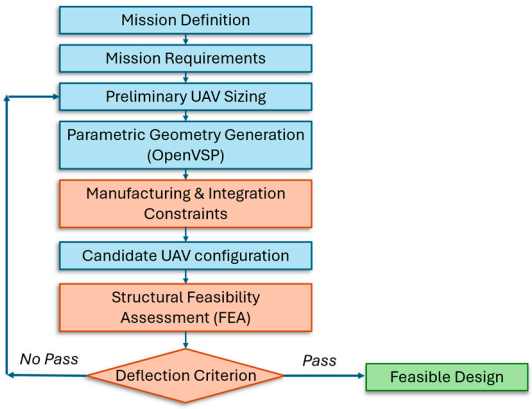


Figure 5. Iterative conceptual design workflow integrating mission sizing, manufacturing constraints, and structural assessment.

Mission requirements derived in Section 2 are initially translated into first-order sizing parameters using conventional conceptual aircraft design relations. These parameters are subsequently used to generate a parametric UAV geometry in OpenVSP, including wingspan, aspect ratio, taper ratio, and fuselage dimensions.

Manufacturing and deployment constraints are introduced directly during the geometry definition stage. These include printable component dimensions, modular wing segmentation, carbon-spar integration, internal subsystem packaging, and detachable interfaces associated with hand-launch and backpackable operation.

Candidate configurations are subsequently evaluated through simplified finite element analysis to assess structural stiffness and overall deformation. The iterative procedure starts from the mission-derived sizing parameters, which define an initial parametric geometry. This geometry is first checked against the manufacturing and deployment constraints listed in Table 3 and is then subjected to the structural feasibility assessment. When a constraint is not satisfied, the parameters directly associated with that constraint—such as component dimensions, wing segmentation, aspect ratio, or internal structural arrangement—are revised and the geometry is regenerated. Manufacturing and deployment constraints are rechecked after each modification, followed by structural reassessment. The iteration is terminated when the resulting configuration simultaneously satisfies the mission-derived sizing requirements, manufacturing and deployment constraints, and the adopted structural feasibility criterion.

During each iteration, the engineering decisions revisited depend on the constraint that is violated. Geometry refinement may involve adjustments to wing span, aspect ratio, taper ratio, or fuselage dimensions, while manufacturing limitations may require changes in wing segmentation and detachable interfaces. Structural refinement primarily concerns the internal load-carrying arrangement and the integration of the carbon-fiber

spar, including its accommodation within the printed wing geometry. These modifications may in turn affect component dimensions, assembly, and packaging; therefore, the updated configuration is rechecked against the manufacturing and deployment constraints before the next structural assessment.

Table 3. Manufacturing and integration constraints considered during conceptual design.

Constraint Category	Constraint Expression	Design Impact
Printer build size/volume	$L_{part} \leq L_{printer}$	Limits the maximum size of printable components
Wing segmentation	$L_{segment} \leq L_{printer}$	Requires modular wing architecture for fabrication and transport
Carbon spar integration (diameters)	$D_{hole} \geq D_{tube} + \Delta_{tol}$	Defines tolerances for spar insertion and internal layout
Printing orientation	$\theta_{print} \approx \theta_{load}$	Aligns print orientation with primary loading direction
Internal subsystem placement	$V_{fuselage} \geq V_{systems}$	Ensures sufficient subsystem packaging volume
Detachable joints	$A_{joint} \geq A_{min}$	Ensures structural integrity of modular joints
Backpack transport	$L_{component} \leq L_{pack}$	Limits the length of disassembled components for field portability

Each stage of the workflow produces a distinct engineering outcome that progressively defines the representative UAV configuration. Mission analysis establishes the operational requirements and sizing targets, while the initial sizing stage identifies the feasible wing- and power-loading region and the corresponding aspect ratio. Preliminary and parametric geometry definition translates these targets into the overall aircraft configuration and component dimensions. The manufacturing and integration stage then determines practical features such as wing segmentation, detachable interfaces, subsystem accommodation, and carbon-spar integration. Finally, the structural assessment provides a stiffness-based feasibility check and identifies whether further geometric or structural refinement is required before a feasible conceptual configuration is accepted.

In this context, the iterative process represents an engineering design refinement procedure rather than a formal numerical optimization algorithm; design variables are modified in response to identified constraint violations until a feasible conceptual configuration is obtained.

3.3. Manufacturing and Integration Constraints

To ensure compatibility with additive manufacturing and modular field deployment, a series of manufacturing and integration constraints were introduced directly into the conceptual design process.

Accordingly, the constraints summarized in Table 3 are treated as active design checks throughout the iterative refinement process rather than as manufacturing requirements applied only after the geometry has been defined. For the representative UAV considered in this study, the generalized constraints of Table 3 were instantiated according to the available manufacturing and integration capabilities. The nominal 256 mm printer build dimension resulted in a practical maximum printable wing-segment length of approximately 250 mm, allowing a small manufacturing clearance. This dimensional restriction directly governed the wing segmentation and, together with carbon-spar integration and the requirement for a detachable and transportable configuration, was among the principal constraints shaping the final architecture. Other requirements, such as subsystem accommodation and printing orientation, were primarily treated as feasibility checks rather than independently governing constraints. These numerical limits are specific to the representative application and are not intrinsic parameters of the proposed methodology.

These constraints include printable component dimensions, modular wing segmentation, spar integration tolerances, printing orientation considerations, internal subsystem

packaging, detachable structural interfaces, and transportation limitations associated with backpackable operation. Similar manufacturing-driven configuration limitations have also been identified in previous additive-manufacturing UAV studies [16,17].

It should be noted that the proposed framework is not restricted to the capabilities of a specific additive manufacturing platform. Recent advances in additive manufacturing, such as continuous or effectively unlimited *Z*-axis printing systems, may reduce or even eliminate limitations associated with the maximum printable component length. However, within the proposed methodology, printer build volume represents only one of several manufacturing-related constraints. Practical engineering considerations, including modularity, transportation, field deployment, assembly, maintenance, and backpack portability, continue to influence the UAV's conceptual configuration regardless of printer size. Consequently, improvements in additive manufacturing capabilities primarily modify the feasible design space by relaxing individual manufacturing constraints, while the overall design methodology remains unchanged. Only the corresponding manufacturing constraints need to be adapted to reflect the capabilities of the selected manufacturing platform.

The constraints directly influence the feasible geometric configuration, internal structural arrangement, and component layout of the UAV. As a result, manufacturability and deployment considerations are incorporated during the conceptual sizing stage rather than treated as secondary design corrections during prototyping and assembly.

Following the conceptual design stage, the complete UAV airframe was fabricated using fused filament fabrication (FFF), with PLA used for the printed structural components and carbon-fiber elements integrated according to the structural configuration. The fabrication stage was used to demonstrate the physical realizability of the resulting configuration rather than to investigate or optimize the additive-manufacturing process itself.

3.4. Parametric Geometry Generation

Parametric geometry generation was performed in OpenVSP, allowing direct coupling between mission-driven sizing parameters and manufacturing-related constraints. The parametric model enabled rapid modification of key geometric variables, including wingspan, aspect ratio, taper ratio, fuselage dimensions, wing segmentation, and detachable structural interfaces.

Additional geometric constraints associated with subsystem packaging and carbon-spar integration were also incorporated during the geometry definition process. This allowed candidate configurations to be evaluated with respect to both aerodynamic sizing requirements and fabrication feasibility within the same conceptual design loop. The resulting configuration therefore reflects not only the aerodynamic sizing targets but also the practical requirements for component segmentation, subsystem accommodation, detachable assembly, and carbon-spar integration.

The resulting geometries were subsequently transferred to the structural assessment phase to evaluate global stiffness behavior and conceptual structural feasibility. If the structural criterion was not satisfied, the relevant geometric or internal structural parameters were revised and the updated geometry was returned to the manufacturing and integration checks. The revised configuration was then structurally reassessed, and this feedback loop was repeated until both the manufacturing/deployment constraints and the structural feasibility criterion were simultaneously satisfied.

4. Structural Analysis and Feasibility Assessment

4.1. Structural Modeling Assumptions

Finite element analysis is employed to assess the structural feasibility of the candidate wing configuration under representative static loading conditions. The analysis focuses

on global stiffness and deformation, providing structural feedback within the conceptual design loop. Dynamic, aeroelastic, and fluid–structure interaction effects are beyond the scope of the present conceptual-level assessment. The loading conditions were derived from the critical flight conditions identified through the V–n assessment. For the representative UAV, a positive design load factor of $n = 4$ was adopted, with a maximum flight speed of 110 km/h and an aircraft mass of approximately 4 kg. The corresponding aerodynamic wing loading was distributed spanwise using Schrenk's approximation. The structural assessment focused on the design flight condition at the positive design load factor. The hand-launch condition was also identified as a relevant operational loading scenario; however, it was not explicitly evaluated in the present FE analysis and is retained for future extension of the structural assessment. Because the analysis aims to provide a conceptual-level structural assessment, we assumed linear elastic material behaviour and quasi-static loading conditions throughout the study.

In order to maintain a computationally efficient model suitable for iterative conceptual design, the internal 3D-printed wing lattice structure was not modeled explicitly. Instead, the printed internal reinforcement was represented through an equivalent increase in skin thickness. The equivalent skin thickness was calibrated against a more detailed wing model including the internal lattice structure under representative loading and boundary conditions. The thickness of the simplified model was iteratively adjusted until comparable global tip-displacement behavior was obtained between the two configurations. The calibration was performed by applying the same 10 N reference load to the detailed internally reinforced model and the simplified equivalent-thickness model and matching their global vertical displacement response. Under this reference load, the detailed internally reinforced model exhibited a maximum vertical displacement of 4.25 mm, compared with 6.07 mm for the initial simplified model. An increase of 0.35 mm in the skin thickness of the simplified model was subsequently required to reproduce the global displacement response of the detailed configuration.

It is acknowledged that the equivalent-thickness representation does not constitute a universally invariant structural equivalence and may vary with geometric modifications and local structural layout. However, within the conceptual design scope of the present study, where the examined configuration variations remain relatively limited, the approach was considered sufficient for reproducing representative global stiffness trends while maintaining computational efficiency during the iterative design process. Accordingly, the analysis focuses primarily on global structural stiffness and displacement behavior rather than local stress concentrations. The carbon-fiber spar was modeled using an equivalent hollow circular beam representation consistent with the actual structural configuration.

4.2. Finite Element Model Description

The finite element model was generated in the CAD environment of ANSYS SpaceClaim (Release 2025 R2) [18]. Basic model verification procedures, including mesh convergence checks, gravitational loading tests, unit displacement cases, and modal analysis, were performed to ensure consistent structural behavior. Mesh convergence was assessed with respect to the maximum wing-tip displacement, which represents the primary structural response quantity used in the present conceptual-level assessment.

The wing root was modeled using fixed support boundary conditions. Aerodynamic loading was estimated using Schrenk's approximation and applied as spanwise distributed forces together with the corresponding pitching moment contribution.

The applied loads were transferred through internal reference nodes connected to the wing skin using multipoint constraint (MPC) relations equivalent to RBE3-type load

distribution. This approach allowed for realistic load transfer without introducing artificial local stiffness into the structural model (Figure 6).

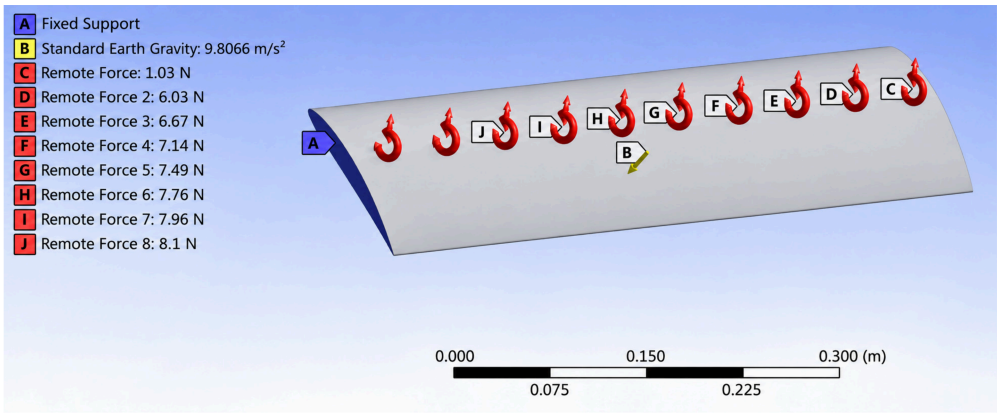


Figure 6. Wing finite element model with loading and boundary conditions.

Representative elastic properties were assigned to the PLA wing structure and carbon-fiber spar for the conceptual-level structural assessment. Both materials were modeled as linear elastic materials, using a Young's modulus of approximately 3 GPa for the printed PLA components and an axial modulus of approximately 70 GPa for the carbon-fiber spar. These values were adopted as representative properties for the simplified FE model, whose purpose is to assess global stiffness and deformation rather than detailed material-level behavior.

4.3. Structural Response and Feasibility Metrics

At the conceptual design stage, structural feasibility was evaluated primarily through a stiffness-based tip deflection criterion under representative static loading conditions. The FE results showed that out-of-plane wing deformation constituted the dominant structural response and therefore provided the governing stiffness measure used to assess the feasibility of the candidate configuration. The maximum wing-tip displacement was constrained according to Equation (2).

$$\delta_{\text{tip,max}} \leq 0.05\, b \tag{2}$$

where $\delta_{\text{tip,max}}$ denotes the maximum wing-tip displacement and b is the wing span. The 5% span criterion was adopted in the present study as a conceptual-level stiffness threshold for screening candidate configurations rather than as a general structural design limit. Its purpose is to provide a consistent displacement-based feasibility criterion within the iterative design process.

Within the proposed framework, the structural assessment acts as an iterative feasibility filter rather than a final structural validation procedure. For the design flight condition at the positive design load factor, the FE model predicted a maximum wing-tip displacement of approximately 39.3 mm, corresponding to approximately 2.9% of the 1.36 m wingspan. This value remained below the adopted 5% span stiffness threshold (68 mm) and was therefore used as the governing displacement response for the conceptual structural-feasibility assessment. The hand-launch condition, although identified as a relevant operational loading scenario, was not explicitly evaluated in the present FE analysis. Configurations that did not satisfy the stiffness criterion were returned to the refinement loop described in Section 3.2, where geometric parameters and the internal structural arrangement were adjusted before reassessment.

Manufacturing and deployment constraints are introduced directly within the conceptual design loop rather than applied retrospectively to an unconstrained configuration.

In the representative application, the nominal 256 mm printer build dimension, corresponding to an approximately 250 mm practical maximum printable component length, directly governed wing segmentation. Carbon-spar integration, detachable interfaces, and transportability requirements further influenced the internal structural arrangement and assembly architecture. Other manufacturing requirements were retained as feasibility checks during the iterative refinement process. Accordingly, the representative application demonstrates how manufacturing and deployment constraints become active within the conceptual design process rather than constituting a comparative optimization between unconstrained and constrained configurations.

5. Conclusions

This work presented a conceptual design framework for small modular UAVs that integrates mission-driven sizing, parametric geometry generation, manufacturing constraints, and simplified structural assessment into a unified iterative design process. The main engineering outcome of this integrated process is the progressive translation of mission requirements into a physically realizable configuration: aerodynamic sizing defines the feasible design region, parametric geometry establishes the aircraft layout, manufacturing constraints determine practical segmentation and integration features, and structural assessment verifies whether the resulting configuration provides adequate conceptual-level stiffness. The proposed methodology incorporates additive manufacturing, subsystem integration, modular assembly, and field-deployment constraints directly during the conceptual design stage. As a result, the framework evaluates candidate configurations not only against aerodynamic and mission requirements, but also against fabrication feasibility and structural stiffness. The framework combines conventional aircraft sizing methods with parametric geometry generation and conceptual finite element assessment in support of rapid UAV prototyping and early-stage configuration evaluation.

The representative UAV considered in this work demonstrates the applicability of the proposed methodology under a specific set of mission, manufacturing, and deployment requirements. It is not intended to establish comparative optimality against alternative UAV configurations. Although the present study is limited to conceptual-level structural assessment, the methodology establishes a practical basis for integrating manufacturing and deployment considerations into early UAV design. Future work will include higher-fidelity structural analysis, detailed subsystem integration, and experimental flight validation.

Author Contributions: Conceptualization, D.S. and E.K.; methodology, D.S. and E.K.; software, D.S. and E.G.; validation, E.K. and E.G.; formal analysis, E.K., E.G. and D.S.; investigation, E.K., E.G. and D.S.; resources, E.G.; data curation, E.K., E.G. and D.S.; writing—original draft preparation, E.K., E.G. and D.S.; writing—review and editing, D.S.; visualization, D.S.; supervision, D.S.; project administration, D.S.; All authors have read and agreed to the published version of the manuscript.

Funding: This research received no external funding.

Institutional Review Board Statement: Not applicable.

Informed Consent Statement: Not applicable.

Data Availability Statement: The data supporting the findings of this study are included in the article. Further inquiries can be directed to the corresponding author.

Acknowledgments: The authors acknowledge the contributions of Hellenic Air Force Academy cadets P. Zikos and P. Theotokatos, who were involved in the project as part of their diploma thesis activities, as well as Th. Lekas for his supervision and academic support. The authors also acknowledge the use of ChatGPT-5.5 for language refinement and editorial assistance during the preparation of this

manuscript. All generated content was critically reviewed and revised by the authors, who take full responsibility for the final published version.

Conflicts of Interest: The authors declare no conflicts of interest.

Appendix A

Appendix A presents the spreadsheet-based conceptual sizing environment developed as part of the first author's doctoral research [19].

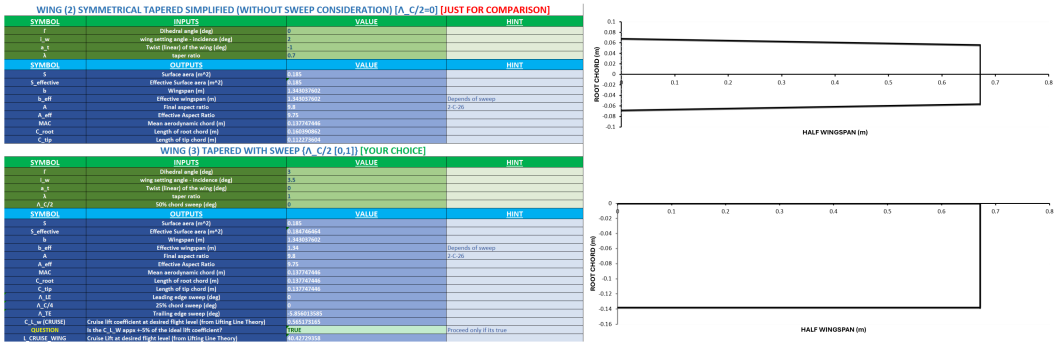


Figure A1. Excel-based conceptual sizing environment used during preliminary UAV design (Wing-Design Phase).

Appendix B

Table A1. Key preliminary stability and configuration parameters.

Parameter	Value
(C_{m_\alpha})	−0.0046
(C_{n_\beta})	0.148
Horizontal tail volume coefficient (V_H)	0.60
Vertical tail volume coefficient (V_V)	0.04
CG position from reference datum	0.230 m
Selected tail configuration	V-tail
Stability condition	Satisfied

References

1. U.S. Department of the Army. *FM 3-0 Operations*; U.S. Department of the Army: Arlington County, VA, USA, 2022.
2. Raymer, D.P. *Aircraft Design: A Conceptual Approach*, 6th ed.; AIAA Education Series; American Institute of Aeronautics and Astronautics, Inc.: Reston, VA, USA, 2018.
3. Roskam, J. *Airplane Design Part I: Preliminary Sizing of Airplanes*; Roskam Aviation and Engineering Corporation: Ottawa, KS, USA, 1985.
4. Sadraey, M.H. *Design of Unmanned Aerial Systems*; Wiley: Hoboken, NJ, USA, 2020. [CrossRef]
5. Sadraey, M.H. *Aircraft Design: A Systems Engineering Approach*; Wiley: Hoboken, NJ, USA, 2013. [CrossRef]
6. Brandt, S.A. Small UAV Design Development and Sizing. In *Handbook of Unmanned Aerial Vehicles*; Valavanis, K., Vachtsevanos, G., Eds.; Springer: Cham, Switzerland, 2018. [CrossRef]
7. Karatzas, E.; Kostopoulos, V.; Lappas, V. Preliminary weight estimation of canister based light foldable wing electric propulsion UAV, as a platform for swarm applications. *J. Phys. Conf. Ser.* **2023**, *2526*, 012082. [CrossRef]
8. Karatzas, E.; Nikolaou, E.; Pitsis, A.; Alexopoulos, S.; Lappas, V.; Kostopoulos, V. Wing Design for Class I Mini Unmanned Aerial Vehicles—Special Considerations for Foldable Wing Configuration at Low Reynolds Numbers. *Eng. Proc.* **2025**, *90*, 96. [CrossRef]
9. Karatzas, E.; Nikolaou, E.; Pitsis, A.; Alexopoulos, S.; Roussos, S.; Georgantakis, E.; Lappas, V.; Kostopoulos, V. Conceptual design and analysis of a tube-launched fixed-wing UAV with integrated folding wing systems. *Aerosp. Sci. Technol.* **2025**, *168*, 111248. [CrossRef]
10. Nikolaou, E.; Kostopoulos, V. Vee-tail preliminary design methodology for Class I mini-UAV. *J. Phys. Conf. Ser.* **2024**, *2716*, 012062. [CrossRef]

11. McDonald, R.A.; Gloudemans, J.R. Open Vehicle Sketch Pad: An Open Source Parametric Geometry and Analysis Tool for Conceptual Aircraft Design. In *AIAA SCITECH 2022 Forum*; American Institute of Aeronautics and Astronautics: Reston, VA, USA, 2022. [CrossRef]
12. OpenVSP. Open Vehicle Sketch Pad, Version 3.40.0. 2024. Available online: https://openvsp.org/blogs/announcements/2024/07/20/openvsp-3-40-0-released (accessed on 23 May 2026).
13. Thompson, M.K.; Moroni, G.; Vaneker, T.; Fadel, G.; Campbell, R.I.; Gibson, I.; Bernard, A.; Schulz, J.; Graf, P.; Ahuja, B.; et al. Design for Additive Manufacturing: Trends, opportunities, considerations, and constraints. *CIRP Ann.-Manuf. Technol.* **2016**, *65*, 737–760. [CrossRef]
14. Pradel, P.; Zhu, Z.; Bibb, R.; Moultrie, J. Investigation of design for additive manufacturing in professional design practice. *J. Eng. Des.* **2018**, *29*, 165–200. [CrossRef]
15. Formentini, G.; Bouissiere, F.; Cuiller, C.; Dereux, P.-E.; Favi, C. Conceptual Design for Assembly methodology formalization: Systems installation analysis and manufacturing information integration in the design and development of aircraft architectures. *J. Ind. Inf. Integr.* **2022**, *26*, 100327. [CrossRef]
16. Klippstein, H.; Diaz De Cerio Sanchez, A.; Hassanin, H.; Zweiri, Y.; Seneviratne, L. Fused Deposition Modeling for Unmanned Aerial Vehicles (UAVs): A Review. *Adv. Eng. Mater.* **2018**, *20*, 1700552. [CrossRef]
17. Šostakaitė, L.; Šapranauskas, E.; Rudinskas, D.; Rimkus, A.; Gribniak, V. Investigating Additive Manufacturing Possibilities for an Unmanned Aerial Vehicle with Polymeric Materials. *Polymers* **2024**, *16*, 2600. [CrossRef] [PubMed]
18. ANSYS, Inc. Ansys SpaceClaim, Release 2025 R2. 2025. Available online: https://ansyshelp.ansys.com/public/Views/Secured/corp/v252/en/pdf/Ansys_Release_Notes.pdf (accessed on 23 May 2026).
19. Karatzas, E. A Design Methodology for Conceptual and Preliminary Design of Electric Class 1 UAS: Application to a Canister-Launched Fixed Wing Platform with Foldable Wing Mechanism. Ph.D. Thesis, University of Patras, Patras, Greece, 2026.

Disclaimer/Publisher's Note: The statements, opinions and data contained in all publications are solely those of the individual author(s) and contributor(s) and not of MDPI and/or the editor(s). MDPI and/or the editor(s) disclaim responsibility for any injury to people or property resulting from any ideas, methods, instructions or products referred to in the content.